How ecosystems recover from pulse perturbations: A theory of short- to long-term responses

Jean-François Arnoldi, Azenor Bideault, Michel Loreau, Bart Haegeman

Journal of Theoretical Biology 436 (2018) 79–92

Contents lists available at ScienceDirect

Journal of Theoretical Biology

journal homepage: www.elsevier.com/locate/jtbi

How ecosystems recover from pulse perturbations: A theory of short- to long-term responses

J.-F. Arnoldi[a], A. Bideault[a,b], M. Loreau[a], B. Haegeman[a,*]

[a] Centre for Biodiversity Theory and Modelling, Theoretical and Experimental Ecology Station, CNRS and Paul Sabatier University, Moulis, France
[b] Integrative Ecology Lab, Département de Biologie, Université de Sherbrooke, Sherbrooke, QC, Canada

ARTICLE INFO

Article history:
Received 2 March 2017
Revised 21 September 2017
Accepted 4 October 2017
Available online 4 October 2017

Keywords:
Ecosystem stability
Return to equilibrium
Asymptotic resilience
Transient dynamics
Reactivity
Rare species

ABSTRACT

Quantifying stability properties of ecosystems is an important problem in ecology. A common approach is based on the recovery from pulse perturbations, and posits that the faster an ecosystem return to its pre-perturbation state, the more stable it is. Theoretical studies often collapse the recovery dynamics into a single quantity: the long-term rate of return, called asymptotic resilience. However, empirical studies typically measure the recovery dynamics at much shorter time scales. In this paper we explain why asymptotic resilience is rarely representative of the short-term recovery. First, we show that, in contrast to asymptotic resilience, short-term return rates depend on features of the perturbation, in particular on the way its intensity is distributed over species. We argue that empirically relevant predictions can be obtained by considering the median response over a set of perturbations, for which we provide explicit formulas. Next, we show that the recovery dynamics are controlled through time by different species: abundant species tend to govern the short-term recovery, while rare species often dominate the long-term recovery. This shift from abundant to rare species typically causes short-term return rates to be unrelated to asymptotic resilience. We illustrate that asymptotic resilience can be determined by rare species that have almost no effect on the observable part of the recovery dynamics. Finally, we discuss how these findings can help to better connect empirical observations and theoretical predictions.

1. Introduction

Ecosystem stability, in particular, the way ecosystems respond to perturbations, is a longstanding topic of interest in ecology (May, 1973; Pimm, 1984; Tilman and Downing, 1994). Ecologists have used a variety of procedures to quantify this type of ecosystem stability, differing in the characteristics of perturbations and in the way the system response is measured. A perturbation can consist of a change in an environmental parameter lasting for short or long times. It can correspond to biomass addition or removal, applied once or repeatedly. The ecosystem response can be assessed soon after the perturbation or much later, measuring the overall state of the ecosystem or an ecosystem variable of specific interest. This multitude of procedures has led to an overabundance of stability measures, whose relationships are often unclear (Donohue et al., 2013; Grimm and Wissel, 1997; Ives and Carpenter, 2007).

We focus here on measures based on an ecosystem's response to pulse perturbations, i.e., perturbations of relatively short duration (Bender et al., 1984). We assume that after a sufficiently long time following a perturbation the ecosystem returns to the pre-perturbed state, which we call equilibrium. We posit that the faster the return the more stable the ecosystem is. Several stability measures can then be defined, differing in the time at which, and the ecosystem variable of which, the return to equilibrium is assessed. Terms used for these measures include return time, recovery rate, and resilience.[1]

Quantifying ecosystem stability using the return to equilibrium is a common approach in both empirical and theoretical studies. Indeed, pulse perturbations are an appropriate model for many natural disturbances, such as floods, forest fires and disease outbreaks, and have been widely applied in experimental ecosystems. In the latter, it is typically the short-term return to equilibrium that is studied, due to practical difficulties of collecting long time series (e.g., Steiner et al., 2006; Downing and Leibold, 2010; Hoover et al., 2014; Wright et al., 2015). This stands in sharp contrast

* Corresponding author.
E-mail addresses: jean-francois.arnoldi@sete.cnrs.fr (J.-F. Arnoldi), azenor.bideault@outlook.fr (A. Bideault), michel.loreau@sete.cnrs.fr (M. Loreau), bart.haegeman@sete.cnrs.fr (B. Haegeman).

https://doi.org/10.1016/j.jtbi.2017.10.003
0022-5193/

[1] The term resilience might lead to confusion, because it is also used for a rather different set of stability measures (Gunderson, 2000; Holling, 1973).

with theoretical work, in which the return to equilibrium is mainly studied at long time scales (e.g., Rooney et al., 2006; Loeuille, 2010; Thébault and Fontaine, 2010; Gellner and McCann, 2016). This is due to the fact that the long-term rate of return to equilibrium, known as asymptotic resilience, can directly be computed from the dominant eigenvalue of the community matrix (we revisit this theory in the next section).

The problem that ecological theory and data do not necessarily address the same time scales has been emphasized before (reviewed in Hastings, 2010). In particular, Neubert and Caswell (1997) argued that the initial response of an ecosystem to a pulse perturbation can strongly differ from its long-term response. They described ecosystems that eventually return to equilibrium for any perturbation but initially move away following some perturbations. Our work can be seen as an extension of Neubert and Caswell's theory. Specifically, while their work dealt with the perturbation that causes the strongest response, we shall study the ecosystem average, or typical, response, and extend the analysis over all time scales.

We begin with a precise definition of return rates and return times covering the range between initial to asymptotic response to a perturbation. We show that short- and long-term return rates differ in their dependence on the perturbation direction, i.e., the way its intensity is distributed over species. This dependence can be strong for short times, but vanishes in the limit of very long times (i.e., asymptotic resilience). To compare short- and long-term return rates on an equal footing, we propose to summarize the distribution of return rates following different perturbations by its median, for which we present a simple and accurate approximation. Using this approach, we find that species abundance can play a predominant role in the recovery dynamics. In particular, rare species (that is, those with low abundance) often have a strong effect on the long-term response, while their effect on the short-term response is typically very weak. We describe the underlying mechanism, and illustrate its generality using a random model of many-species competitive communities.[2] Our results show that asymptotic resilience and short-term return rates are typically disconnected. While asymptotic resilience provides only a partial view on the recovery dynamics, empirically relevant predictions can be obtained from short-term return rates, such as those introduced and studied in this paper.

2. Defining return rates and return times

The study of the recovery dynamics starts by specifying the state from which the ecosystem is perturbed and to which it returns after the perturbation. Empirically, this reference state is a dynamic equilibrium, characterized by relatively small fluctuations around a fixed average. The pulse perturbation then induces a much larger displacement, such that the ecosystem leaves its reference state, thus initiating the recovery dynamics.

It is practically impossible to study the recovery once the displacement induced by the perturbation has become indistinguishable from the fluctuations of the dynamic equilibrium. This is a common problem in the analysis of empirical time series. Yet, almost all theoretical work focuses on the long-term return, which is, in principle, observable only if equilibrium fluctuations are absent. In other words, theory typically assumes the reference state to be a static equilibrium (May, 1973, 1974), a fixed point of a deterministic dynamical system. We also make this assumption, emphasizing however that our results on the short-term recovery also hold for a fluctuating reference state.

Denoting the vector of dynamical variables (e.g., the biomass of the species in the ecosystem) by $\boldsymbol{N}(t)$ and the equilibrium point by $\boldsymbol{N}^*$, we focus on the dynamics for the displacement vector $\boldsymbol{x}(t) = \boldsymbol{N}(t) - \boldsymbol{N}^*$. A pulse perturbation applied at time $t = 0$ to the ecosystem previously at equilibrium (i.e., $\boldsymbol{x}(t) = 0$ for $t < 0$) is characterized by a vector $\boldsymbol{u}$ and describes the ecosystem's state immediately after the perturbation (i.e., $\boldsymbol{x}(0^+) = \boldsymbol{u}$). For pulse perturbations that are not too strong, a linearization of the dynamics around the equilibrium yields a qualitatively accurate, yet analytically tractable, picture of the recovery dynamics (we come back to this assumption and its limitations in the discussion). These linearized dynamics are governed by the community matrix A, that is, the Jacobian of the non-linear dynamical equations evaluated at $\boldsymbol{N}^*$,

$$\frac{\mathrm{d}\boldsymbol{x}}{\mathrm{d}t} = A\boldsymbol{x}. \tag{1}$$

Eq. (1) yields the recovery trajectory $\boldsymbol{x}(t)$ following the pulse perturbation,

$$\boldsymbol{x}(t) = \mathrm{e}^{At}\boldsymbol{u} \quad \text{for } t > 0, \tag{2}$$

where e^A denotes the matrix exponential of A. We assume the equilibrium to be stable in the sense of the stability criterion, so that the system returns to equilibrium following any sufficiently small displacement, so that $\lim_{t\to\infty} \boldsymbol{x}(t) = 0$.

We are interested in quantifying how stable the system is, based on the idea that a more stable system returns faster to equilibrium. This general idea can be implemented in several ways. Here we introduce one classic measure that will serve as a reference throughout. It is based on the asymptotic return to equilibrium,

$$\mathcal{R}_\infty = \lim_{t\to\infty} -\frac{\ln \|\boldsymbol{x}(t)\|}{t}, \tag{3}$$

where the Euclidean norm $\|\boldsymbol{x}(t)\| = \sqrt{\sum_i x_i^2(t)}$ measures the phase-space distance to equilibrium. Eq. (3) states that $\|\boldsymbol{x}(t)\|$ decays asymptotically as $\mathrm{e}^{-\mathcal{R}_\infty t}$. In principle, $\mathcal{R}_\infty$ could depend on the perturbation vector $\boldsymbol{u}$. However, $\mathcal{R}_\infty$ is in fact the same for virtually any perturbation $\boldsymbol{u}$ (see Appendix A). This common value, called asymptotic resilience, is equal to $-\Re\mathrm{e}(\lambda_{\mathrm{dom}}(A))$, where $\lambda_{\mathrm{dom}}(A)$ is the eigenvalue of A with the largest real part.[3]

Return rates. While the asymptotic return yields a stability measure with elegant mathematical properties, only the finite-time recovery is of practical interest. We define two finite-time return rates: the instantaneous return rate at time t,

$$\mathcal{R}_t^{\mathrm{ins}} = -\frac{1}{\|\boldsymbol{x}(t)\|}\frac{\mathrm{d}\|\boldsymbol{x}(t)\|}{\mathrm{d}t} = -\frac{\mathrm{d}}{\mathrm{d}t}\ln\|\boldsymbol{x}(t)\|, \tag{4}$$

and the average return rate over the interval $[0, t]$,

$$\mathcal{R}_t^{\mathrm{avg}} = -\frac{\ln\|\boldsymbol{x}(t)\| - \ln\|\boldsymbol{x}(0^+)\|}{t}. \tag{5}$$

Definitions (4) and (5) are illustrated in Fig. 1, where we apply a pulse perturbation to a two-species community at equilibrium. From the recovery dynamics of variables $N_1(t)$ and $N_2(t)$, we deduce the distance to equilibrium $\|\boldsymbol{x}(t)\|$ as a function of time (panel A). To construct the return rates $\mathcal{R}_t^{\mathrm{ins}}$ and $\mathcal{R}_t^{\mathrm{avg}}$, we plot this distance on a logarithmic scale (panel B). The instantaneous return rate $\mathcal{R}_t^{\mathrm{ins}}$ at time t is the slope (with opposite sign) of this curve at time t. The average return rate $\mathcal{R}_t^{\mathrm{avg}}$ at time t is the slope (with opposite sign) of the segment connecting the distances to equilibrium at times 0 and t. Those rates can substantially differ; they

[2] Note, however, that our theory does not require any assumptions on interaction types.

[3] The stability criterion is equivalent to $\Re\mathrm{e}(\lambda_{\mathrm{dom}}(A)) < 0$, so that $\mathcal{R}_\infty$ is positive for stable systems.

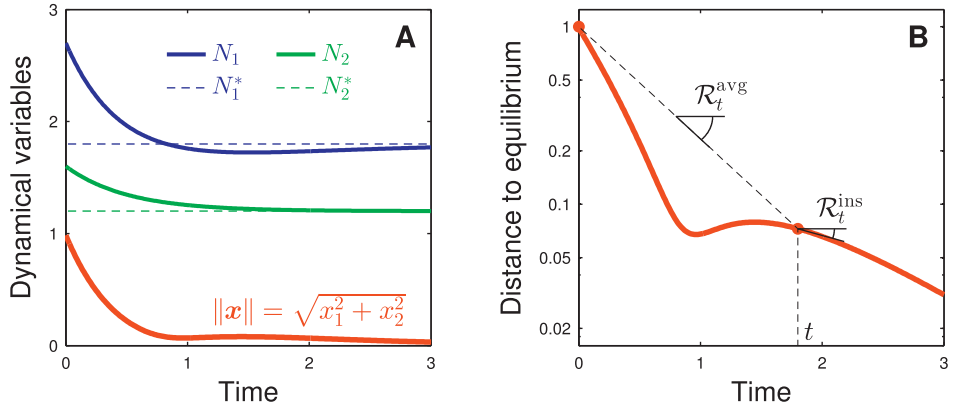

Fig. 1. Definition of return rates. The response of an ecological system to a pulse perturbation contains information about the system's stability, as illustrated here for a system of two interacting species. Panel A: We apply a pulse perturbation after which the species biomass $N_1(t)$ (blue) and $N_2(t)$ (green) return to their equilibrium values N_1^* and N_2^*. We monitor the recovery dynamics by the distance to equilibrium (red), $\|\boldsymbol{x}(t)\| = \sqrt{x_1^2(t) + x_2^2(t)}$ with $x_i(t) = N_i(t) - N_i^*$. Panel B: The relative rate at which the distance to equilibrium diminishes is a commonly used stability measure (note the logarithmic scale on the y-axis). Here we distinguish between the average rate of return $\mathcal{R}_t^{\mathrm{avg}}$ over the period $[0, t]$, and the instantaneous rate of return $\mathcal{R}_t^{\mathrm{ins}}$ at time t. These two measures can largely differ, and can even have opposite sign. Parameter values: $\boldsymbol{N}^{*\top} = (1.8, 1.2)$, $A = \left(\begin{smallmatrix} -1 & -4 \\ 0 & -2 \end{smallmatrix}\right)$ and $\boldsymbol{u}^\top = (0.9, 0.4)$. (For interpretation of the references to color in this figure legend, the reader is referred to the web version of this article.)

can even have opposite sign. For example, in Fig. 1, at time $t \approx 1.2$, we have $\mathcal{R}_t^{\mathrm{ins}} < 0$ and $\mathcal{R}_t^{\mathrm{avg}} > 0$ meaning that the trajectory moves away from equilibrium at that time, while having come closer to equilibrium since the end of the perturbation.

It is instructive to compare the behavior of return rates $\mathcal{R}_t^{\mathrm{ins}}$ and $\mathcal{R}_t^{\mathrm{avg}}$ for very small and very large times t. It holds generally that $\mathcal{R}_0^{\mathrm{ins}} = \lim_{t\to 0} \mathcal{R}_t^{\mathrm{avg}}$ and that $\lim_{t\to\infty} \mathcal{R}_t^{\mathrm{avg}} = \mathcal{R}_\infty$. However, the analogous relationship $\lim_{t\to\infty} \mathcal{R}_t^{\mathrm{ins}} = \mathcal{R}_\infty$ does not always hold. It does for the example of Fig. 1, but does not for the one of Fig. A.1 (Appendix A). In the latter, return rate $\mathcal{R}_t^{\mathrm{ins}}$ continues to oscillate between positive and negative values for large time t, so that $\mathcal{R}_t^{\mathrm{ins}}$ does not tend to a steady value. This is avoided when considering a time-average of $\mathcal{R}_t^{\mathrm{ins}}$, such as $\mathcal{R}_t^{\mathrm{avg}}$. This is one reason why we shall focus on average return rates $\mathcal{R}_t^{\mathrm{avg}}$. Finally, it should be noted that while the theory in this paper is based on the distance to equilibrium, it can be extended to other ecosystem variables (see Appendix B).

Return times. While return rates measure the speed at which an ecosystem approaches equilibrium, it might be more interesting to consider the time it takes for an ecosystem to recover from a perturbation, i.e., its return time. Return rates and return times are clearly related. Return time is defined as the amount of time between the perturbation and the instant at which the distance to equilibrium becomes smaller than a prespecified bound. In Appendix C we show that this yields a family of return times parameterized by this bound, and we describe how these return times are related to average return rates $\mathcal{R}_t^{\mathrm{avg}}$. This provides another reason why we shall mainly focus on the latter. If the bound is chosen as the typical extent of the fluctuations in the equilibrium state, then the return time corresponds to the time during which the ecosystem response is distinguishable from equilibrium fluctuations.

In theoretical studies the return time is often approximated as the reciprocal of asymptotic resilience. This approach, initiated by Pimm and Lawton (1977, 1978), is not self-evident as it uses the asymptotic regime to describe the entire recovery dynamics. It implicitly assumes that the asymptotic return rate is a good proxy for the return rates at shorter times. As we argue extensively below, this need not be the case. It is in fact more appropriate to quantify the return time as the reciprocal of a finite-time return rate. For this matter the average return rate $\mathcal{R}_t^{\mathrm{avg}}$ is particularly well suited, as it is based on the same part of the recovery that controls return times.

3. Return rates depend on perturbation direction

As mentioned above, virtually any pulse perturbation leads to the same asymptotic rate of return to equilibrium. Due to this remarkable property, asymptotic resilience has been called an intrinsic stability measure (Arnoldi et al., 2016). In contrast, finite-time return rates do depend on features of the perturbation; they are not fully determined by the system dynamics. Restricting to linear systems, we now investigate this qualitative difference.

A pulse perturbation along a perturbation vector $\boldsymbol{u}$ causes a displacement $\boldsymbol{x}(0^+) = \boldsymbol{u}$. By linearity, the perturbation intensity, quantified by the norm $\|\boldsymbol{u}\|$, has a trivial effect: when the perturbation is multiplied by a constant factor, the response is multiplied by the same factor, which therefore does not affect return rates. We may thus restrict our attention to normalized vectors $\|\boldsymbol{u}\| = 1$, i.e., perturbation *directions*. In ecological terms, the direction $\boldsymbol{u}$ defines the way the perturbation intensity is distributed over the constituent species of the ecosystem.

We focus on the average return rates $\mathcal{R}_t^{\mathrm{avg}}$ but the results are similar for the other stability measures introduced in the previous section. Recall that $\lim_{t\to\infty} \mathcal{R}_t^{\mathrm{avg}} = \mathcal{R}_\infty$, and let us denote the initial return rate by $\mathcal{R}_0 = \lim_{t\to 0} \mathcal{R}_t^{\mathrm{avg}}$.

We start with a simple example of two non-interacting species (Fig. 2). The community matrix $A = \left(\begin{smallmatrix} -4 & 0 \\ 0 & -1 \end{smallmatrix}\right)$ indicates that the first species responds four times faster to a displacement than the second. The species with the slowest recovery determines asymptotic resilience $\mathcal{R}_\infty = 1$, thus following an arbitrary perturbation the system eventually returns to equilibrium with unit rate (Fig. 2B). This asymptotic rate is, however, not informative about the short-term recovery. In particular, the system absorbs a perturbation that mainly affects the first species (perturbation 'a' in Fig. 2) much faster than a perturbation that mainly affects the second species (perturbation 'b' in Fig. 2).

As a result, at small t, the distribution of possible return rates $\mathcal{R}_t^{\mathrm{avg}}$ (associated to all possible perturbation directions) is quite broad, but becomes increasingly narrow at longer times t (see Fig. 2D). Asymptotic resilience, which is the lower limit of each of these distributions, is not a good predictor of the short-term return rate for an arbitrary perturbation.

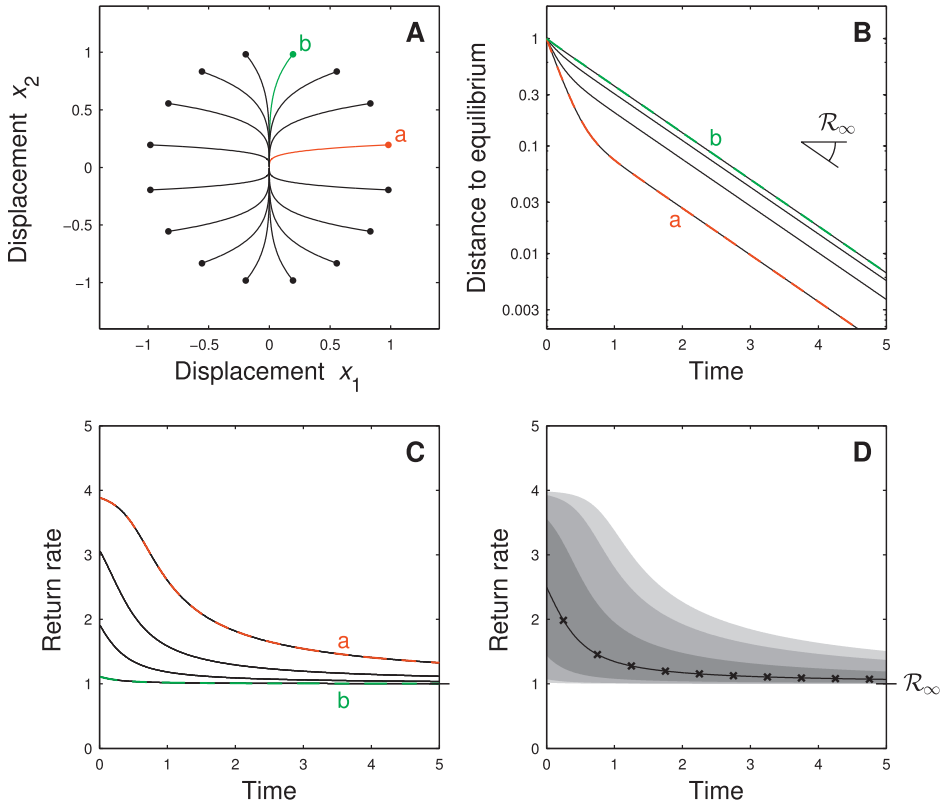

Fig. 2. Return to equilibrium depends on perturbation direction - non-reactive case. Two-species system with community matrix $A = \left(\begin{smallmatrix} -4 & 0 \\ 0 & -1 \end{smallmatrix}\right)$, that is, species 1 responds four times faster than species 2. Panel A: phase-plane trajectories (lines) for several perturbations $\boldsymbol{u} = \boldsymbol{x}(0^+)$ (dots). For instance, perturbation 'a' (red) affects mostly species 1, while perturbation 'b' (green) affects mostly species 2. Note that all perturbations have the same intensity $\|\boldsymbol{u}\| = 1$. Panel B: dynamics of distance to equilibrium $\|\boldsymbol{x}(t)\|$ for the perturbations of panel A. Perturbation 'a' in red, perturbation 'b' in green and the other perturbations in black (several of them coincide). The return to equilibrium is faster for perturbation 'a' than for perturbation 'b'. For all perturbations the distance to equilibrium eventually decays at a rate given by asymptotic resilience $\mathcal{R}_\infty$. Panel C: return rate $\mathcal{R}_t^{\text{avg}}$ as a function of time for the perturbations of panel A. As expected, the return rates are initially almost four times larger for perturbation 'a' than for perturbation 'b'. Panel D: statistics of return rate $\mathcal{R}_t^{\text{avg}}$ for random perturbations (fixed intensity, uniformly distributed). Full line: median computed from simulations; $\times$-marks: analytical approximation for median; shades of gray: 5%, 10%, 25%, 75%, 90% and 95% percentiles. (For interpretation of the references to color in this figure legend, the reader is referred to the web version of this article.)

Consider now the asymmetric community matrix $A = \left(\begin{smallmatrix} -1 & -4 \\ 0 & -2 \end{smallmatrix}\right)$. Although all trajectories eventually return to equilibrium at a rate $\mathcal{R}_\infty = 1$, the short-term return to equilibrium has a much richer behavior (Fig. 3B). Many trajectories have short-term return rates either well above asymptotic resilience, or much smaller and even negative return rates (thus moving away from equilibrium). The latter phenomenon occurs because the system is reactive (Neubert and Caswell, 1997), which guarantees that there exist trajectories for which $\mathcal{R}_0 < 0$. However, it does not exclude that other trajectories display positive initial return rates. In fact, for the system in Fig. 3 the distribution of $\mathcal{R}_0$ is mainly concentrated on positive values (Fig. 3D).

In general, the distribution of return rates $\mathcal{R}_t^{\text{avg}}$ over time has a funnel shape: a broad distribution for small times t and an increasingly narrow distribution for larger times. This can be understood from the initial and asymptotic return rates $\mathcal{R}_0$ and $\mathcal{R}_\infty$. The distribution of $\mathcal{R}_0$ depends on all the eigenvalues of the symmetric part of the community matrix (Appendix D). Because these eigenvalues can span a large range, the distribution of $\mathcal{R}_0$ is typically wide. In contrast, $\mathcal{R}_\infty$ only depends on one eigenvalue of the community matrix. The distribution of return rates $\mathcal{R}_t^{\text{avg}}$ for $0 < t < \infty$ connects these two extremes, yielding the characteristic funnel shape. In Appendix D we show that other stability measures based on return rates exhibit similar patterns.

4. Averaging over perturbation directions

In practice, we can rarely know how a perturbation, whether natural or experimentally induced, will displace the ecosystem state variables. Here we propose a minimalistic way to deal with this uncertainty. We model the perturbation direction as a random variable, so that the return trajectories are also random. Each realization corresponds to a particular perturbation, which initiates a single return trajectory. To obtain a relevant prediction, we average the system response over the perturbation directions. Specifically, we construct a 'typical' return trajectory by taking, at each time after the perturbation, an average over the perturbation directions. This typical trajectory is not necessarily the response to a particular perturbation. Rather, it is the composition of the average displacements through time.

In Appendix D we derive simple and accurate formulas for the median system response, given a community matrix A and statistics of the random perturbation $\boldsymbol{u}$ encoded in a covariance matrix C. Component C_{ii} of this matrix is the variance of initial displacement u_i of species i. Component C_{ij} is the covariance of u_i and u_j; this covariance accounts for the fact that species i and j may undergo similar initial displacements. These formulas for median distance to equilibrium and return rate are

$$\mathbb{M}\left(\|\boldsymbol{x}(t)\|\right) \approx \sqrt{\mathrm{Tr}\left(e^{At}\, C\, e^{A^\top t}\right)} \tag{6a}$$

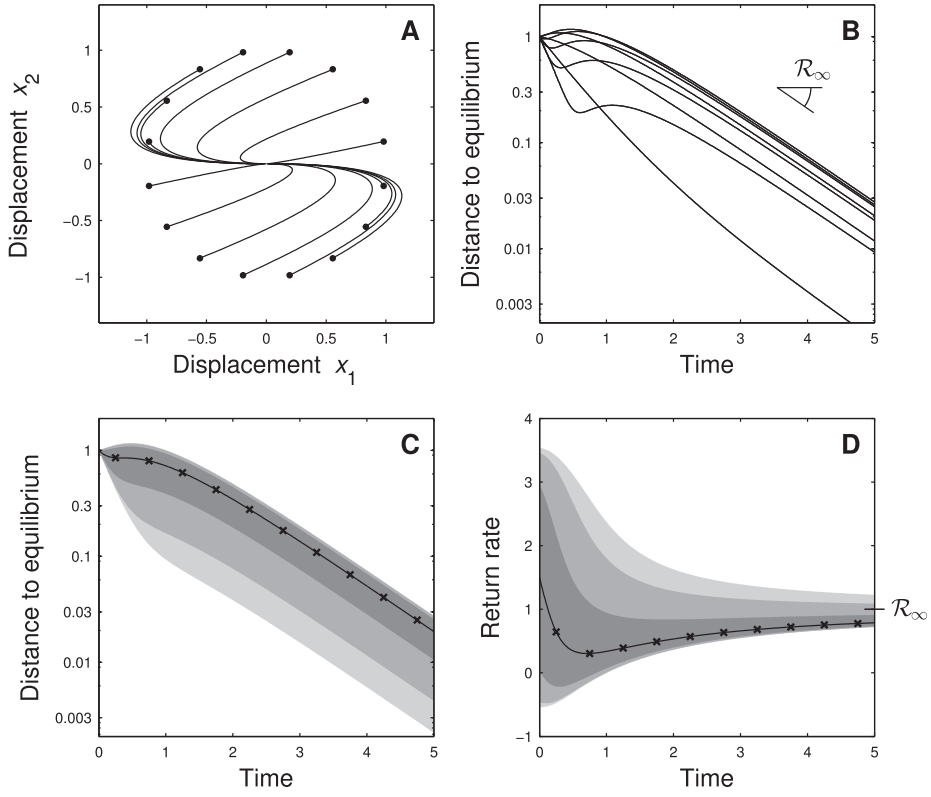

Fig. 3. Return to equilibrium depends on perturbation direction - reactive case. Two-species system with community matrix $A = \left(\begin{smallmatrix} -1 & -4 \\ 0 & -2 \end{smallmatrix}\right)$. Panel A: phase-plane trajectories for several perturbations $\boldsymbol{u}$. Panel B: dynamics of distance to equilibrium. For some perturbations the system initially moves away from the equilibrium, but for all perturbations the distance to equilibrium eventually decays at a rate equal to asymptotic resilience $\mathcal{R}_\infty$. Panels C and D: statistics of distance to equilibrium and of return rate $\mathcal{R}_t^{\text{avg}}$ for random perturbations (fixed intensity, uniformly distributed). Full line: median computed from simulations; $\times$-marks: analytical approximation for median; shades of gray: 5%, 10%, 25%, 75%, 90% and 95% percentiles.

$$\mathbb{M}\left(\mathcal{R}_t^{\text{avg}}\right) \approx -\frac{\ln \text{Tr}\left(e^{At}\, C\, e^{A^\top t}\right) - \ln \text{Tr}(C)}{2t}, \tag{6b}$$

where the symbol $\mathbb{M}$ stands for the median over the ensemble of perturbation directions.

To illustrate their accuracy, we apply equations (6) to a few examples, first revisiting those of Figs. 2 and 3. We assume here that the perturbation directions are uniformly distributed. This assumption corresponds to setting the perturbation covariance matrix C proportional to the identity matrix ($C_{ii} = 1/n$ and $C_{ij} = 0$, with n the number of species in the system; see Appendix E). The agreement between the numerically computed medians (full line) and their analytical approximations ($\times$-marks) is excellent (see Figs. 2D, 3C and 3D).

In the absence of additional information, the uniform distribution is an appropriate model for the perturbation randomness. As previously explained, in the linear regime, only the perturbation directions affect return rates and there is no reason to prefer one direction over another. However, additional information does exist in the form of the equilibrium biomasses N_i^*. When species biomasses substantially differ, the distribution over perturbation directions should be non-uniform.

To make this point clear, let us take a numerical example. Suppose a perturbation acts on a two-species system, in which the first species is ten times more abundant than the second ($N_1^* = 10\, N_2^*$). Compare perturbation 'a' that mostly displaces species 1 (e.g., $u_1 = 10\, u_2$) and perturbation 'b' that mostly displaces species 2 (e.g., $u_1 = 0.1\, u_2$) as depicted in Fig. 2. Perturbation 'a' affects both species equally in relative terms, while perturbation 'b' has a very strong effect on the rare species (in relative but also in absolute terms). Clearly, perturbation 'a' is more likely than perturbation 'b'. This implies that the distribution over perturbations directions should assign a larger weight to perturbation 'a' than to perturbation 'b'. This requirement disqualifies the uniform distribution as a suitable perturbation model.

There is no unique perturbation model in the case of an uneven abundance distribution. Here we propose to take the expected displacement u_i of species i proportional to its equilibrium biomass N_i^*. That is, all species are perturbed equally in relative terms. In Appendix E we prove that this assumption corresponds to setting the perturbation covariance matrix C to $C_{ii} = (N_i^*)^2/\Lambda$ and $C_{i\neq j} = 0$, with $\Lambda = \sum_i (N_i^*)^2$. If all species have the same equilibrium biomass, we recover the formula for uniformly distributed perturbation directions. We use this biomass-dependent perturbation model in all the examples below.[4]

In Fig. 4 we revisit the example of Fig. 2, assuming that species have different equilibrium biomass. The biomass of species 1, which recovers four times faster than species 2, is ten times larger than the biomass of species 2. Due to its larger biomass, species 1 is typically displaced more strongly than species 2. Hence, the perturbations are no longer uniformly distributed (as was the case previously, see Fig. 2A), but are concentrated close to the x_1-axis corresponding to species 1 (see Fig. 4A). This implies that the fast recovery of species 1 has a much larger contribution to the average system recovery than in the previous scenario. For example, the median distance to equilibrium drops to about 5% of the initial displacement at the fast return rate of species 1 (Fig. 4C, for

[4] One could also integrate additional information, such as a higher or lower vulnerability to perturbations of particular species, and positive or negative correlations in the responses of certain pairs of species.

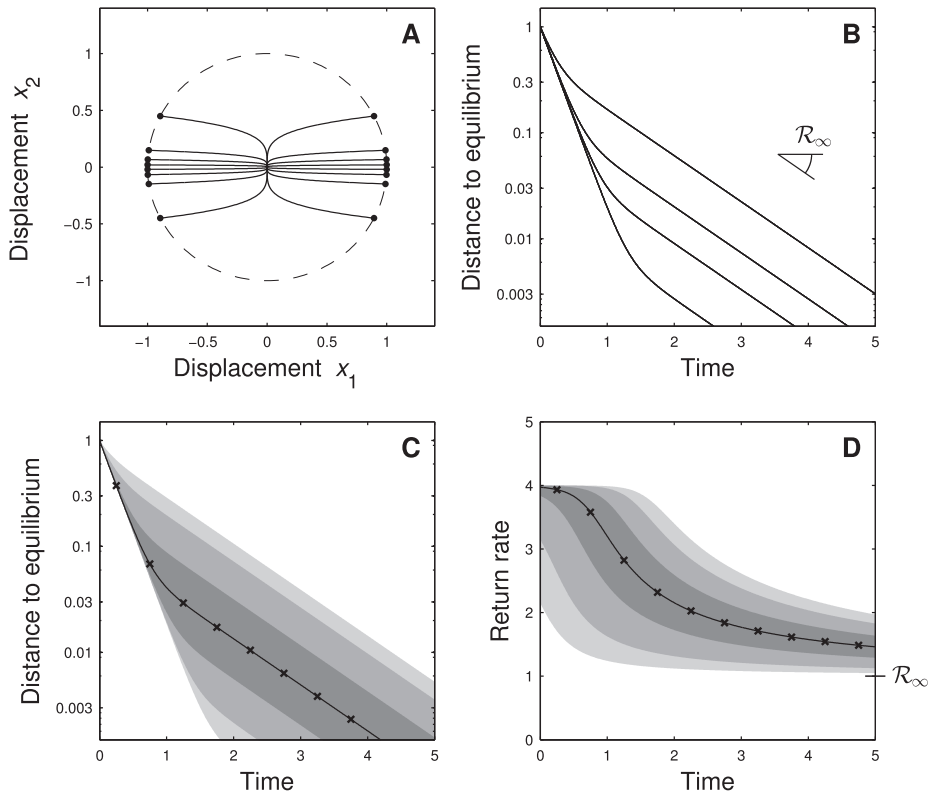

Fig. 4. Return to equilibrium for biomass-dependent perturbations. Same system as Fig. 2, but here we take into account that perturbations affect abundant and rare species differently. Specifically, we assume that the equilibrium biomass of species 1 (the species with the fastest response) is ten times larger than the equilibrium biomass of species 2. Panel A: phase-plane trajectories for several perturbations $\boldsymbol{u}$. Perturbations are no longer spread out on the unit circle (dashed line), but tend to be directed along the x_1-axis corresponding to species 1 (dots). Panel B: dynamics of distance to equilibrium. For most perturbations the distance to equilibrium becomes small (below 10% of the pulse perturbation) at a rate equal to the return rate of species 1 (rather than the return rate of species 2, which is equal to asymptotic resilience). Panels C and D: statistics of distance to equilibrium and of return rate $\mathcal{R}_t^{\text{avg}}$, taking into account that perturbations tend to displace species 1 more strongly than species 2. As a result, perturbations like the one labeled 'a' in Fig. 2 contribute more strongly to the statistics than perturbations like the one labeled 'b' in Fig. 2.

times $t < 1$). The slow return rate of species 2, equal to asymptotic resilience, governs the ecosystem response only later.

5. Effect of rare species on recovery dynamics

As illustrated in Fig. 4, rare species can dominate the ecosystem response in the long term. This happens because rare species have the potential to introduce slow return rates in the system dynamics, and hence to determine asymptotic resilience. Here we explain why we expect this phenomenon to be common in real-world communities.

We emphasize that there is no mathematically inevitable link between species rarity and long-term return rates. This can easily be shown by considering a system of non-interacting species, whose biomasses N_i obey logistic growth with intrinsic growth rate r_i and carrying capacity K_i:

$$\frac{\mathrm{d}N_i}{\mathrm{d}t} = r_i N_i \left(1 - \frac{N_i}{K_i}\right), \tag{7}$$

In the absence of interactions, each eigenvalue λ_i of the linearized community dynamics can be attributed to a different species as $\lambda_i = -r_i$. Hence different parameters determine equilibrium biomass (K_i) and eigenvalue ($-r_i$). By choosing parameters appropriately, any species can provide the dominant eigenvalue, irrespective of its abundance.

Thus, the claim that rare species govern the long-term recovery cannot hold in full generality. However, it can be expected as a common trend. To show this, we focus our attention on a particular type of rare species, namely those that play a minor role in the community. We call these species *satellite*, in opposition to *core* species, which constitute the bulk of the community biomass. This terminology is borrowed from Hanski (1982), who introduced it to describe the regional distribution of species, whereas we apply it to the local level. Removing satellite species does not impinge on community functioning. Satellite species do not affect core species, or only weakly, but can be strongly affected by them. In particular, competition with core species prevents them from reaching higher abundances. Natural communities almost always contain numerous rare species, and while some of them might be an essential part of the community, a large majority can be expected to be satellite.

Despite their minor role in the community, satellite species can be predominant in the long-term return dynamics. To understand why this is the case, consider the following thought experiment, illustrated in Fig. 5. Suppose that all core species are aggregated into a single biomass variable coupled to a single satellite species (see Appendix F for details). If the satellite species is absent or cannot persist, the return rate is constant and determined by the core species (Fig. 5, green line, case A). If the satellite species can persist, however, it modifies the recovery dynamics (Fig. 5, red line, case B). The short-term recovery is not affected, but once the distance to equilibrium has decayed to a small fraction ($\approx 5\%$) of the initial displacement, the return to equilibrium becomes much slower, corresponding to the asymptotic resilience of the coupled core-satellite system. In natural communities species are often maintained by immigration, especially rare ones. Thus, suppose that the satellite species is now maintained in the community by immigration (i.e., a sink population). As be-

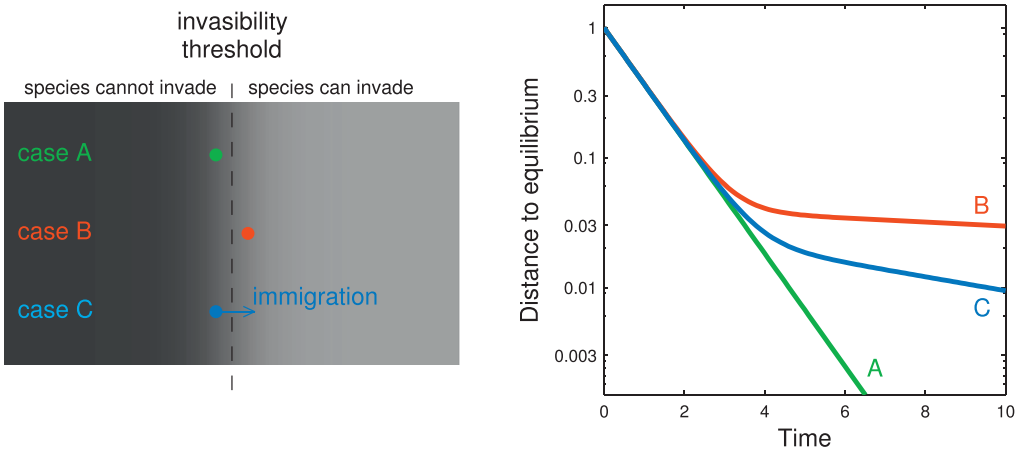

Fig. 5. Effect of rare species on the long-term return to equilibrium. We study a simplified core-satellite competitive system, describing the introduction of a satellite species into an established community. Case A: if the introduced species has invasion fitness just below the invasibility threshold, it cannot persist and the dynamics are those of the core species alone (green line in right-hand panel). Case B: if the introduced species has invasion fitness just above the invasibility threshold, it persists at a small equilibrium biomass. Compared to the community without the satellite species, the short-term return to equilibrium does not change, but the long-term return to equilibrium becomes much slower (red line in right-hand panel). Case C: we assume weak immigration, maintaining the introduced species at a small equilibrium biomass (source-sink dynamics). As in case B, the long-term return to equilibrium is much slower (blue line in right-hand panel). Model details and parameter values are given in Appendix F. (For interpretation of the references to color in this figure legend, the reader is referred to the web version of this article.)

fore, the presence of the satellite species does not affect the short-term recovery, but it drastically slows down the long-term recovery (Fig. 5, blue line, case C). Again, the part governed by asymptotic resilience sets in only very close to equilibrium, and is therefore of limited practical interest.

This thought experiment can be formalized in terms of the eigenvalues of the linearized dynamics, before and after introducing the satellite species. Because the satellite species has a negligible effect on the core community, the dynamics of the latter are essentially unaffected, and the eigenvalues of the core community alone are still eigenvalues of the coupled system. The latter has one additional eigenvalue, associated with the dynamics of the satellite species. This eigenvalue can introduce a slow return rate (i.e., have small negative real part), especially if the satellite species is close to the invasibility threshold (see Fig. 5 and Appendix F), and thus yield the dominant eigenvalue of the whole system. In this case, asymptotic resilience is determined by a single rare species and contains limited information about community stability.

Each satellite species can provide the dominant eigenvalue, and we expect that real-world communities contain many such species. Hence, the influence of rare species on the long-term recovery dynamics should be widespread. We provide support for this claim using a random model of many-species competitive communities. We impose that the equilibrium community has a realistic (log-normal) abundance distribution, with numerous rare species. The dynamics of species biomasses N_i are governed by Lotka–Volterra equations,

$$\frac{\mathrm{d}N_i}{\mathrm{d}t} = N_i\left(a_i - \sum_{j=1}^{n} b_{ij}N_j\right) \quad \text{for } i = 1,\ldots,n. \tag{8}$$

Parameter values of the $n = 10$ species are chosen as follows. First, we randomly generate the species biomasses N_i^* using a broken-stick model (MacArthur, 1957; Sugihara, 1980). We divide the total biomass $\sum_i N_i^* = 1$ over the species by first allocating a random fraction (uniformly in the interval [0, 1]) of the total biomass to the first species, then by allocating a random fraction (uniformly in the interval [0, 1]) of the remaining biomass to the second species, and so on. Second, we randomly draw the competition coefficients b_{ij}: the intraspecific competition coefficients b_{ii} from the uniform distribution on the interval [0.5, 1], and the interspecific competition coefficients b_{ij} with $i \neq j$ from the uniform distribution on the interval [0, 0.5]. Third, we determine the intrinsic growth rates a_i such that the species biomasses N_i^* correspond to an equilibrium, that is, $a_i = \sum_j b_{ij}N_j^*$. We check whether this equilibrium is stable, and discard the model realization if this is not case[5].

The distribution of the recovery trajectories are shown in Fig. 6A. At time $t = 100$ most trajectories have decayed to a small fraction ($\approx 5\%$) of the initial displacement. This level of displacement is typically no longer observable in noisy time series. However, the return rate continues to decrease, from $\mathcal{R}_{100}^{\mathrm{avg}}$ with median 0.02 to $\mathcal{R}_\infty$ with median 0.0002 (Fig. 6B; note that the median $\mathcal{R}_\infty$ corresponds to a horizontal line in Fig. 6A). By inspecting individual model realizations, we see that the disparity between $\mathcal{R}_{100}^{\mathrm{avg}}$ and $\mathcal{R}_\infty$ is often associated with a rare species. In particular, when removing this species, the recovery dynamics up to time $t = 100$ do not change, while asymptotic resilience does (Fig. F.1). This is consistent with case B of Fig. 5. Hence, asymptotic resilience is determined by the specificities of rare species, which have almost no effect on the observable part of the recovery dynamics. This is further illustrated in Fig. 6C, where we show that, surprisingly, return rates $\mathcal{R}_{100}^{\mathrm{avg}}$ and $\mathcal{R}_\infty$ have a weakly negative correlation. Although this negative correlation is due to the particular model parameterization (and is not generally valid), it clearly illustrates that asymptotic resilience is an unreliable predictor for empirically relevant return rates.

6. Discussion

The theory of ecosystems' response to pulse perturbations developed in this article reveals a fundamental and generic interplay between time-scales and species abundances. While short-term recovery is typically governed by the more abundant species, the return dynamics for longer times tend to be determined by rare species. This shift from abundant to rare species follows from two

[5] This occurs for 23% of the model realizations.

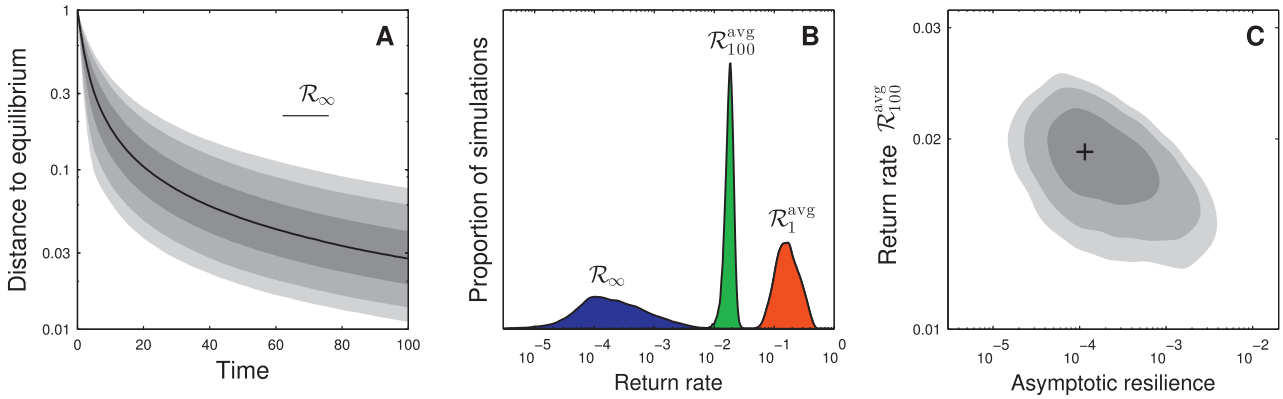

Fig. 6. Return to equilibrium in a random community model. We analyze a Lotka–Volterra model with random competitive interactions. The equilibrium species biomass distribution is generated by the broken-stick model (see main text). Panel A: statistics of distance to equilibrium for random model realizations (averaged over perturbation direction). Black line: median; shades of gray indicate 5%, 10%, 25%, 75%, 90% and 95% percentiles. Median asymptotic resilience $\mathcal{R}_\infty$ corresponds to a virtually horizontal line (represented in the top-right part of the panel). Panel B: probability distribution of return rates $\mathcal{R}_1^{\text{avg}}$, $\mathcal{R}_{100}^{\text{avg}}$ and $\mathcal{R}_\infty$. Asymptotic resilience $\mathcal{R}_\infty$ is orders of magnitude smaller than the finite-time return rates. Panel C: joint probability distribution of return rates $\mathcal{R}_{100}^{\text{avg}}$ and $\mathcal{R}_\infty$. Black cross: maximum; shades of gray indicate regions of 50%, 80% and 90% probability (corresponding to contour lines of the probability distribution). Asymptotic resilience $\mathcal{R}_\infty$ is unreliable as a proxy for return rate $\mathcal{R}_{100}^{\text{avg}}$. For this random community model there is even a (weakly) negative correlation between $\mathcal{R}_{100}^{\text{avg}}$ and $\mathcal{R}_\infty$. The probability distributions in panels B and C were reconstructed using kernel density estimation on 10^4 simulations.

observations. First, a pulse perturbation is expected to initially generate the largest biomass changes in the abundant species, simply because they have larger biomass to begin with. Second, after sufficiently long time, the recovery process becomes independent of the perturbation; it is then determined by the least stable species (in the sense of being closest to the invasibility threshold, see Fig. 5), which is often rare. The fact that distinct sets of species determine the short-term and long-term return rates implies that these two types of return rate are often unrelated, and that the asymptotic response can be determined by the specificities of rare species, which have almost no effect on the observable part of the recovery dynamics.

As a corollary, the asymptotic rate of return to equilibrium, or asymptotic resilience, should not be used as a proxy for the short-term recovery. Nevertheless, theoretical work on the return to equilibrium has focused almost exclusively on asymptotic resilience. For example, return time is often defined as the reciprocal of asymptotic resilience (a practice that dates back to Pimm and Lawton, 1977, 1978). But this theoretical construct need not be related to the actual return time, that is, the time it takes for the system to recover from a perturbation, which is mainly determined by the short-term response. Many ecologists seem to have built an intuition about the return to equilibrium based on very simple systems, such as single species, for which the return rate is constant over time. However, as illustrated by the examples in this paper, only slightly more complex systems exhibit much richer return dynamics, during which the return rate can change dramatically. We showed that in large, complex communities, due to the presence of species with very different abundances, asymptotic resilience need not even be a good predictor of return rates at longer times. Similarly, because asymptotic resilience does not depend on the perturbation direction, many ecologists seem to assume that the same holds for the entire recovery process. This intuition is erroneous because, as we have shown, the short-term return rates can, and often do, strongly depend on the perturbation direction.

Previous work has stressed that the asymptotic regime is often not representative of the short-time dynamics (Hastings, 2004, 2010). This issue has been particularly well studied in population ecology. It is generally recognized that depending on initial conditions the population dynamics can be governed by transient effects, which are missed out when analyzing the asymptotic regime alone (Caswell, 2001; Ezard et al., 2010). Practical tools are available to systematically investigate the transient dynamics of population models, and to incorporate these transient effects into predictions of future population dynamics (Caswell, 2007; Stott et al., 2011). Clearly, there are close parallels with the findings reported in this paper. It would be worthwhile to scrutinize whether theoretical insights and practical tools developed by population ecologists can enrich the study of ecosystem stability.

Because our work emphasizes the importance of the short-term recovery, it is closely related to the work of Neubert and Caswell (1997). They studied the instantaneous return rate immediately after a pulse perturbation, and showed that it can be negative even if the system is stable. They coined the term 'reactive' to denote systems for which this phenomenon occurs, and argued that many real-world systems can be expected to be reactive. However, we have shown that the initial return rate displays a particularly strong dependence on the perturbation direction. Therefore, the existence of a perturbation with a negative initial return rate does not imply that the initial return rate is negative for all or even most perturbations. For instance, in Fig. 3, the vast majority of perturbations are met with positive initial return rates, despite the system being reactive[6]. This suggests that the system property of being reactive does not provide much information about the initial return rate for an actual perturbation. The theory of reactive systems deals with the initial return rate for the worst-case perturbation, but does not tell us how the system typically responds to a perturbation. By studying this typical response, our paper can be interpreted as an extension of Neubert and Caswell's theory.

This paper strives to develop theory for empirically relevant stability measures. The long-term return to equilibrum is of limited practical interest, because it corresponds to small displacements, which are often indistinguishable from inevitable fluctuations at the equilibrium state. Also, especially in field studies, the asymptotic response to a first perturbation might be concealed by the occurrence of a second one. Therefore, available empirical data are often restricted to the short-term recovery, which is explicitly addressed by our theory. Short-term responses depend on the perturbation direction, and we argued that the most relevant predictions are obtained by averaging over the perturbation distribution. We

[6] In fact we show in Appendix D that the median initial return rate is always positive and larger than asymptotic resilience, both for non-reactive and reactive systems.

derived accurate formulas for the median return rate as a function of the time elapsed since the perturbation. These formulas can be evaluated as easily as asymptotic resilience, to which the median return rate converges in the limit of very long times. Thus, our work provides a theoretical framework to study the transient recovery following perturbations and to predict return times to equilibrium in community and ecosystem models.

This theoretical framework depends on a number of technical assumptions. First, we assumed that the reference state, i.e., the state in which the ecosystem settles at the end of the recovery process, is an equilibrium point. Alternatively, and more realistically, we could consider a fluctuating reference state. If the fluctuations are small compared with the displacement induced by the pulse perturbation, then they do not affect the analysis of the short-term recovery. More generally, we assumed that the recovery trajectories remain close to equilibrium. This allowed us to rely on the theory of linear dynamical systems, which are widely used by both theorists and empiricists to describe and interpret ecological dynamics (Caswell, 2001; Gurney and Nisbet, 1998). For sufficiently weak perturbations, the non-linear part of ecosystem dynamics is often an additional source of discrepancy between short-term and long-term responses. Indeed, non-linearities can have a strong effect on the short-term response, but leave the long-term response essentially unchanged, because the latter corresponds to small displacements for which the linear approximation is accurate. When allowing for stronger perturbations, the ecosystem might be pushed to a different state (e.g., to another equilibrium), and the notion of ecosystem recovery itself becomes meaningless (for concrete proposals of how to deal with this case, see Menck et al., 2013 and Lundström, 2017). Finally, it should be noted that ecosystem stability has also been analyzed in the absence of perturbations. For example, many studies have quantified stability based on the amplitude of endogenous oscillations (such as predator-prey cycles; e.g., Brose et al., 2006; McCann et al., 1998 and McCann, 2011), for which our work does not seem directly relevant.

The integration of theoretical and empirical approaches has been identified as one of the main challenges for research on ecological stability (Ives and Carpenter, 2007) and Donohue et al., 2016. This article attempts to make the theory of how ecosystems recover from pulse perturbations more practically relevant by emphasizing short-term responses. Future work could address how to translate our findings into concrete recommendations. While restricted to pulse perturbations, our paper might inspire analogous studies for other stability measures, such as the response to press perturbations and the temporal variability of ecosystems (see Arnoldi et al., 2016 and Haegeman et al., 2016 for first steps in this direction).

Acknowledgements

We thank José Montoya for very helpful discussions, Michael Cortez and an anonymous reviewer for constructive comments on the manuscript. This work was supported by the TULIP Laboratory of Excellence (ANR-10-LABX-41) and by the BIOSTASES Advanced Grant, funded by the European Research Council under the European Union's Horizon 2020 research and innovation programme (grant agreement No 666971).

Appendix

"Bra-ket" notation In the appendices we use special notation to deal with column vectors, row vectors and their products. The correspondence between this notation, which is borrowed from theoretical physics, and the more standard one is:

column vector	$\boldsymbol{x}$	$\lvert\boldsymbol{x}\rangle$
row vector	$\boldsymbol{w}^\top$	$\langle\boldsymbol{w}\rvert$
scalar product	$\boldsymbol{w}^\top\boldsymbol{x}$	$\langle\boldsymbol{w}\rvert\boldsymbol{x}\rangle$
rank-one matrix	$\boldsymbol{x}\boldsymbol{w}^\top$	$\lvert\boldsymbol{x}\rangle\langle\boldsymbol{w}\rvert$

For example, the equality $\boldsymbol{w}^\top A\boldsymbol{x} = \boldsymbol{w}^\top(A\boldsymbol{x}) = (A^\top\boldsymbol{w})^\top\boldsymbol{x}$ corresponds to $\langle\boldsymbol{w}|A|\boldsymbol{x}\rangle = \langle\boldsymbol{w}|A\boldsymbol{x}\rangle = \langle A^\top\boldsymbol{w}|\boldsymbol{x}\rangle$ in the new notation.

Appendix A. Generic perturbations lead to the same asymptotic return rate

Here we show that the asymptotic return rates are essentially independent of the perturbation direction $\boldsymbol{u}$ and of the observation direction $\boldsymbol{w}$.

We begin by investigating the long-term behavior of $\langle\boldsymbol{w}, \boldsymbol{x}(t)\rangle = \langle\boldsymbol{w}, \mathrm{e}^{At}\boldsymbol{u}\rangle$. We assume that A has no degenerate eigenvalues, which is generically the case. This ensures that its spectral decomposition exists, constructed using the eigenvalues λ_i and corresponding (right) eigenvectors $\boldsymbol{v}_i^{\mathrm{R}}$ and left eigenvectors $\boldsymbol{v}_i^{\mathrm{L}}$ (i.e., eigenvectors of $A^\top$). For simplicity we assume that the dominant eigenvalue is real; we discuss the case of a complex conjugate pair of dominant eigenvalues at the end of this appendix. We order the eigenvalues such that

$$\lambda_1 > \mathfrak{Re}(\lambda_2) \geq \mathfrak{Re}(\lambda_3) \geq \dots$$

Using the spectral decomposition, we have

$$A = \sum_i \lambda_i |\boldsymbol{v}_i^{\mathrm{R}}\rangle\langle\boldsymbol{v}_i^{\mathrm{L}}| \quad \text{and} \quad \mathrm{e}^{At} = \sum_i \mathrm{e}^{\lambda_i t}|\boldsymbol{v}_i^{\mathrm{R}}\rangle\langle\boldsymbol{v}_i^{\mathrm{L}}|,$$

so that

$$\langle\boldsymbol{w}|\boldsymbol{x}(t)\rangle = \langle\boldsymbol{w}|\mathrm{e}^{At}\boldsymbol{u}\rangle = \sum_i \mathrm{e}^{\lambda_i t}\langle\boldsymbol{w}|\boldsymbol{v}_i^{\mathrm{R}}\rangle\langle\boldsymbol{v}_i^{\mathrm{L}}|\boldsymbol{u}\rangle.$$

If $\langle\boldsymbol{w}|\boldsymbol{v}_1^{\mathrm{R}}\rangle\langle\boldsymbol{v}_1^{\mathrm{L}}|\boldsymbol{u}\rangle \neq 0$ and for sufficiently large t (more precisely, for $\mathrm{e}^{-(\lambda_1 - \mathfrak{Re}(\lambda_2))t} \ll 1$), the sum in the right-hand side is dominated by the $i = 1$ term,

$$\langle\boldsymbol{w}|\boldsymbol{x}(t)\rangle \approx \mathrm{e}^{\lambda_1 t}\langle\boldsymbol{w}|\boldsymbol{v}_1^{\mathrm{R}}\rangle\langle\boldsymbol{v}_1^{\mathrm{L}}|\boldsymbol{u}\rangle,$$

so that (see also Appendix B),

$$-\frac{\ln|\langle\boldsymbol{w}|\boldsymbol{x}(t)\rangle|}{t} \approx -\lambda_1 - \frac{\ln|\langle\boldsymbol{w}|\boldsymbol{v}_1^{\mathrm{R}}\rangle\langle\boldsymbol{v}_1^{\mathrm{L}}|\boldsymbol{u}\rangle|}{t} \approx -\lambda_1$$

$$\mathcal{R}_t^{\mathrm{ins}}(\boldsymbol{w}) = -\frac{\mathrm{d}}{\mathrm{d}t}\ln|\langle\boldsymbol{w}|\boldsymbol{x}(t)\rangle| \approx -\lambda_1 - \frac{\mathrm{d}}{\mathrm{d}t}\ln|\langle\boldsymbol{w}|\boldsymbol{v}_1^{\mathrm{R}}\rangle\langle\boldsymbol{v}_1^{\mathrm{L}}|\boldsymbol{u}\rangle| = -\lambda_1$$

$$\mathcal{R}_t^{\mathrm{avg}}(\boldsymbol{w}) = -\frac{\ln|\langle\boldsymbol{w}|\boldsymbol{x}(t)\rangle| - \ln|\langle\boldsymbol{w}|\boldsymbol{x}(0)\rangle|}{t} \approx -\lambda_1.$$

These approximations, valid for large t, become exact in the limit $t \to \infty$. Hence,

$$\mathcal{R}_\infty(\boldsymbol{w}) = \lim_{t\to\infty}\mathcal{R}_t^{\mathrm{ins}}(\boldsymbol{w}) = \lim_{t\to\infty}\mathcal{R}_t^{\mathrm{avg}}(\boldsymbol{w}) = -\lambda_1.$$

Hence, the asymptotic return rates do not depend on the perturbation direction $\boldsymbol{u}$ (as long as $\langle\boldsymbol{v}_1^{\mathrm{L}}|\boldsymbol{u}\rangle \neq 0$) and on the observation direction $\boldsymbol{w}$ (as long as $\langle\boldsymbol{w}|\boldsymbol{v}_1^{\mathrm{R}}\rangle \neq 0$).

Similarly, for sufficiently large t and if $\langle\boldsymbol{v}_1^{\mathrm{L}}|\boldsymbol{u}\rangle \neq 0$,

$$\|\boldsymbol{x}(t)\| \approx \mathrm{e}^{\lambda_1 t}\,\|\boldsymbol{v}_i^{\mathrm{R}}\|\,\langle\boldsymbol{v}_i^{\mathrm{L}}|\boldsymbol{u}\rangle.$$

Substituting this expression into the defintion of return rates $\mathcal{R}_\infty$, $\mathcal{R}_t^{\mathrm{ins}}$ and $\mathcal{R}_t^{\mathrm{avg}}$, we get

$$\mathcal{R}_\infty = \lim_{t\to\infty}\mathcal{R}_t^{\mathrm{ins}} = \lim_{t\to\infty}\mathcal{R}_t^{\mathrm{avg}} = -\lambda_1.$$

The case of a complex conjugate pair of dominant eigenvalues is more subtle. In this case also the asymptotic return to equilibrium is governed by the dominant pair of eigenvalues (and corresponding eigenvectors). The asymptotic regime has persistent oscillations of decreasing amplitude. The rate of decrease of the amplitude is equal to asymptotic resilience (equal to minus the real part of the

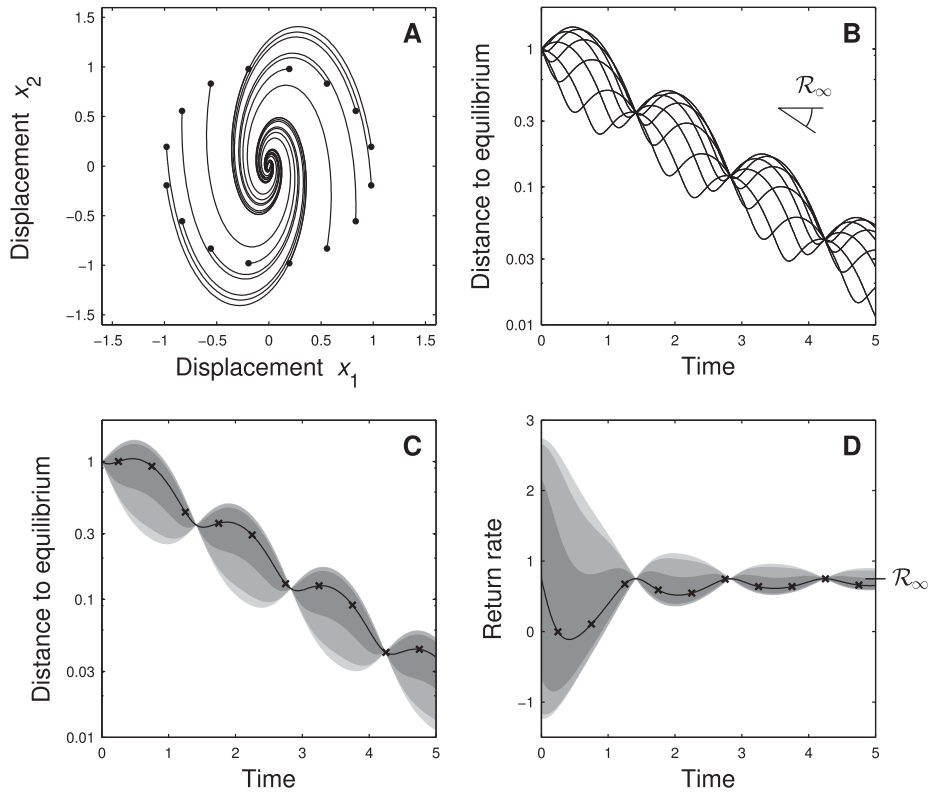

Fig. A.1. Return to equilibrium depends on perturbation direction - case of complex conjugate pair of dominant eigenvalues. Same figure as Fig. 3, but for different community matrix, $A = \begin{pmatrix} -0.5 & -1 \\ 5 & -1 \end{pmatrix}$. The oscillatory behavior leaves a clear imprint on the decay of the distance to equilibrium (panel C) and on the convergence of return rate $\mathcal{R}_t^{\text{avg}}$ to asymptotic resilience (panel D).

dominant eigenvalues). However, because the return rates are computed on the oscillating variables (rather than on the amplitude of the oscillations), the return rates for large t can also oscillate, without converging to a proper limit. The distribution of instantaneous return rates $\mathcal{R}_t^{\text{ins}}$ remains wide for large time t (Fig. A.1). In contrast, the average return rates $\mathcal{R}_t^{\text{avg}}$ have a distribution that becomes narrow for large time t, converging to asymptotic resilience.

Appendix B. Direction of observation

In the main text we defined return rates using the Euclidean norm $\|\boldsymbol{x}(t)\|$ to measure the extent of the dynamical displacement from equilibrium, see Eqs. (3)–(5). To compute the associated return rates, all dynamical variables $x_i(t)$ have to be observed. When this is not practical or even possible, it is more convenient to use return rates that require a limited number of dynamical variables. Here we introduce return rates of a particular ecosystem variable of function (e.g., total biomass, nutrient uptake). After linearization such a variable becomes a linear combination $\sum_i w_i x_i(t) = \boldsymbol{w}^\top \boldsymbol{x} = \langle \boldsymbol{w} | \boldsymbol{x} \rangle$, where the vector $\boldsymbol{w}$ can be interpreted as an observation direction. For instance, the direction of total biomass is $\boldsymbol{w}^\top = (1, 1, \ldots, 1)$. The corresponding return rates are

$$\mathcal{R}_\infty(\boldsymbol{w}) = \lim_{t\to\infty} -\frac{\ln|\langle \boldsymbol{w}|\boldsymbol{x}(t)\rangle|}{t} \tag{B.1}$$

$$\mathcal{R}_t^{\text{ins}}(\boldsymbol{w}) = -\frac{\mathrm{d}}{\mathrm{d}t}\ln|\langle \boldsymbol{w}|\boldsymbol{x}(t)\rangle| \tag{B.2}$$

$$\mathcal{R}_t^{\text{avg}}(\boldsymbol{w}) = -\frac{\ln|\langle \boldsymbol{w}|\boldsymbol{x}(t)\rangle| - \ln|\langle \boldsymbol{w}|\boldsymbol{x}(0^+)\rangle|}{t}. \tag{B.3}$$

Note that we have added the dependence on the observation direction $\boldsymbol{w}$ to distinguish these return rates (e.g., $\mathcal{R}_t^{\text{avg}}(\boldsymbol{w})$) from those based on the Euclidean norm (e.g., $\mathcal{R}_t^{\text{avg}}$).

Appendix C. Return times

As explained in the main text, return time can be defined as the amount of time it takes for the system to return, and remain within, a specified distance to equilibrium. We denote the allowed distance to equilibrium by c. Then, the return time $T(c)$ is defined as

$$T(c) = \min\left\{t \;\middle|\; \|\boldsymbol{x}(t+s)\| \le c \text{ for all } s \ge 0\right\}. \tag{C.1}$$

Fig. C.1 illustrates how the requirement that the displacement remains within this bound for all times $t \ge T(c)$ allows us to deal with non-monotonous return to equilibrium. It is interesting to note that the inverse function $T(c)$ has a simple interpretation. It is the maximal displacement $C(t)$ that occurs after time t,

$$C(t) = \max_{s\ge t} \|\boldsymbol{x}(s)\|. \tag{C.2}$$

The relationship between $T(c)$ and $C(t)$ is explained graphically in Fig. C.1.

Neither $T(c)$ nor $C(t)$ are directly comparable to return rates $\mathcal{R}_t^{\text{ins}}$ and $\mathcal{R}_t^{\text{avg}}$. To see this, note that $T(c)$ has units of time, while $C(t)$ is unitless (recall that $\mathcal{R}_t^{\text{ins}}$ and $\mathcal{R}_t^{\text{avg}}$ have units of reciprocal time). This shortcoming can be overcome by applying an appropriate transformation to $T(c)$ and $C(t)$. To find this transformation, we consider a single-species system, for which $A = -\alpha$ with $\alpha > 0$ and $\mathcal{R}_t^{\text{ins}} = \mathcal{R}_t^{\text{avg}} = \alpha$. We find $C(t) = x(0^+)\,\mathrm{e}^{-\alpha t}$ and $T(c) = -\big(\ln c - \ln x(0^+)\big)/\alpha$, suggesting the following transformed quanti-

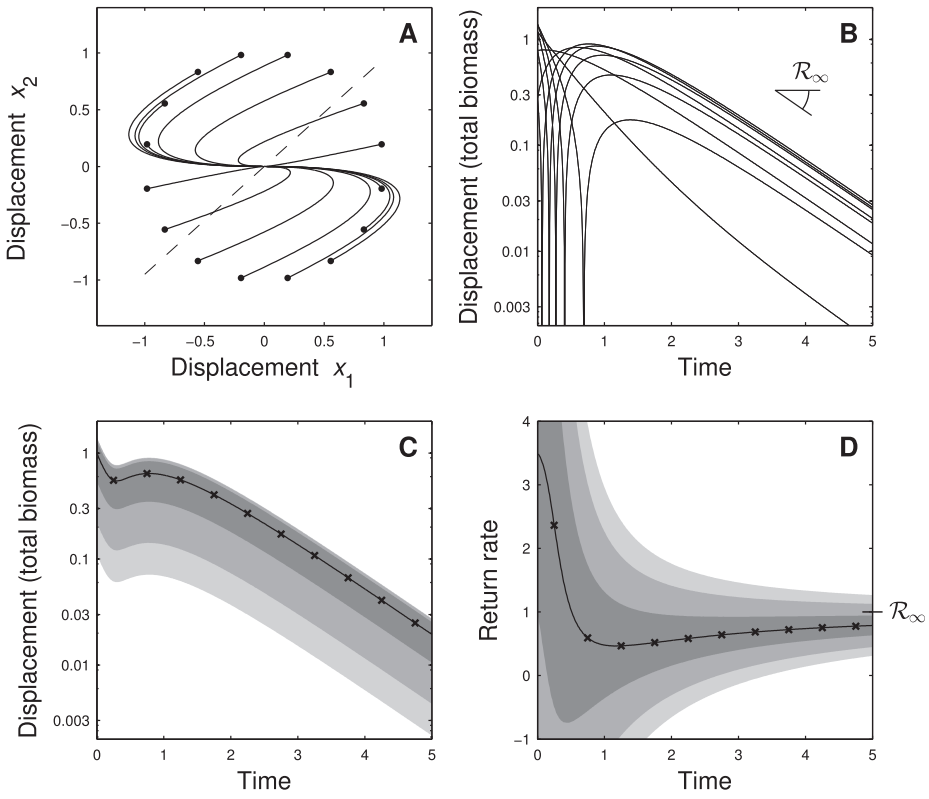

Fig. B.1. Return to equilibrium depends on perturbation direction - displacement measured along a particular observation direction. Same figure as Fig. 3, but the displacement from equilibrium is measured as the deviation of total biomass from its equilibrium value. This corresponds to projecting the trajectories on the observation direction $\boldsymbol{w}^\top = (1, 1)$ (dashed line in panel A). The patterns are qualitatively the same as those in Fig. 3, but the variation around the median is larger.

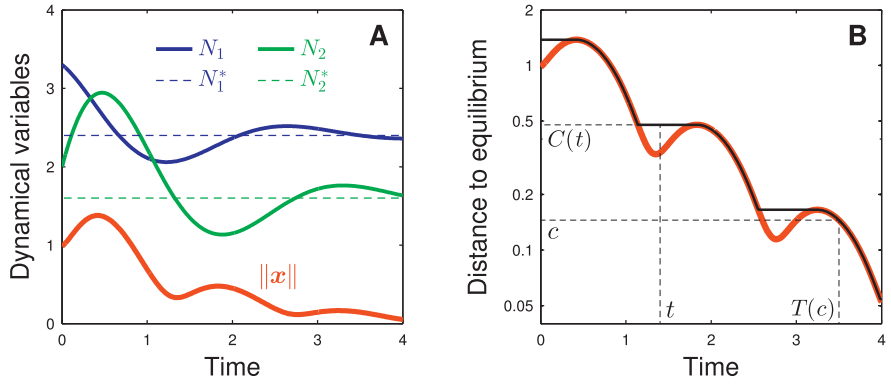

Fig. C.1. Definition of return times. Panel A: same as Fig. 1, but for a return to equilibrium with damped oscillations. Panel B: we define the return time $T(c)$ as the smallest time starting from which the distance to equilibrium remains smaller than a factor c of the initial displacement $\|\boldsymbol{x}(0^+)\|$. To construct the return time, it is convenient to introduce the quantity $C(t)$ as the largest displacement after time t relative to the initial displacement. The function $C(t)$ is monotonously decreasing; its inverse is the return time $T(c)$. Parameter values: $\boldsymbol{N}^{*\top} = (2.4, 1.6)$, $A = \left(\begin{smallmatrix} -0.5 & -1 \\ 5 & -1 \end{smallmatrix}\right)$ and $\boldsymbol{u}^\top = (0.9, 0.4)$.

ties,

$$\mathcal{C}_t = -\frac{\ln C(t) - \ln \|\boldsymbol{x}(0^+)\|}{t} \quad \text{and} \quad \mathcal{T}_c = -\frac{\ln c - \ln \|\boldsymbol{x}(0^+)\|}{T(c)}, \tag{C.3}$$

which have the dimension of reciprocal time. For the purpose of comparison, stability measure $\mathcal{C}_t$ is of particular interest, because it is indexed by time t like return rates $\mathcal{R}_t^{\text{ins}}$ and $\mathcal{R}_t^{\text{avg}}$. Substituting the definition of $C(t)$, we get

$$\mathcal{C}_t = -\frac{\ln \max_{s \geq t} \|\boldsymbol{x}(s)\| - \ln \|\boldsymbol{x}(0^+)\|}{t},$$

showing that $\mathcal{C}_t$ is closely related to $\mathcal{R}_t^{\text{avg}}$. They are equal when $\max_{s \geq t} \|\boldsymbol{x}(s)\| = \|\boldsymbol{x}(t)\|$, which holds when the return to equilibrium is monotonous. This indicates that our results, although mostly expressed in terms of return rate $\mathcal{R}_t^{\text{avg}}$, are also valid for stability measures based on return times such as $\mathcal{C}_t$.

Appendix D. Median return rate

We derive approximate expressions for the median value of return rates $\mathcal{R}_t^{\text{ins}}$ and $\mathcal{R}_t^{\text{avg}}$ for a random perturbation $\boldsymbol{u}$. The only information the approximation requires about the distribution of perturbation vectors $\boldsymbol{u}$ is a correlation matrix C. In the next section

we compute this correlation matrix for a few simple perturbation models.

We start by deriving some exact expressions for averages over the distribution of perturbation vectors. First, we consider the squared displacement from equilibrium. Denoting by $\mathbb{E}$ the mean over the distribution of vectors $\boldsymbol{u}$, we have

$$\begin{aligned}\mathbb{E}\left(\|\boldsymbol{x}(t)\|^2\right) &= \mathbb{E}\,\langle \boldsymbol{x}(t)|\boldsymbol{x}(t)\rangle \\ &= \mathbb{E}\,\langle \mathrm{e}^{At}\boldsymbol{u}|\mathrm{e}^{At}\boldsymbol{u}\rangle \\ &= \mathbb{E}\left(\mathrm{Tr}\,|\mathrm{e}^{At}\boldsymbol{u}\rangle\langle \mathrm{e}^{At}\boldsymbol{u}|\right) \\ &= \mathrm{Tr}\,\mathrm{e}^{At}\,\mathbb{E}\left(|\boldsymbol{u}\rangle\langle\boldsymbol{u}|\right)\mathrm{e}^{A^\top t} \\ &= \mathrm{Tr}\,\mathrm{e}^{At}C\,\mathrm{e}^{A^\top t}, \end{aligned} \tag{D.1}$$

where $C = \mathbb{E}\,|\boldsymbol{u}\rangle\langle\boldsymbol{u}|$ is the correlation matrix of perturbation vectors.

Next, we consider the time derivative of the squared displacement from equilibrium. We have

$$\begin{aligned}\frac{\mathrm{d}}{\mathrm{d}t}\|\boldsymbol{x}(t)\|^2 &= \frac{\mathrm{d}}{\mathrm{d}t}\langle \mathrm{e}^{At}\boldsymbol{u}|\mathrm{e}^{At}\boldsymbol{u}\rangle \\ &= \langle A\boldsymbol{x}(t)|x(t)\rangle + \langle \boldsymbol{x}(t)|A\boldsymbol{x}(t)\rangle \\ &= 2\langle \boldsymbol{x}(t)|H(A)\boldsymbol{x}(t)\rangle, \end{aligned}$$

where $H(A) = (A + A^\top)/2$ is the symmetric part of matrix A. Taking the mean over the perturbation vectors $\boldsymbol{u}$,

$$\begin{aligned}\mathbb{E}\left(\frac{\mathrm{d}}{\mathrm{d}t}\|\boldsymbol{x}(t)\|^2\right) &= 2\,\mathbb{E}\,\langle \boldsymbol{x}(t)|H(A)\boldsymbol{x}(t)\rangle \\ &= 2\,\mathbb{E}\left(\mathrm{Tr}\,|H(A)\,\mathrm{e}^{At}\boldsymbol{u}\rangle\langle \mathrm{e}^{At}\boldsymbol{u}|\right) \\ &= 2\,\mathrm{Tr}\,H(A)\,\mathrm{e}^{At}\,\mathbb{E}\left(|\boldsymbol{u}\rangle\langle\boldsymbol{u}|\right)\mathrm{e}^{A^\top t} \\ &= 2\,\mathrm{Tr}\,H(A)\mathrm{e}^{At}C\,\mathrm{e}^{A^\top t}. \end{aligned} \tag{D.2}$$

We are interested in averages of $\|\boldsymbol{x}(t)\|$, $\mathcal{R}_t^{\mathrm{ins}}$ and $\mathcal{R}_t^{\mathrm{avg}}$. These quantities can be expressed as non-linear functions of $\|\boldsymbol{x}(t)\|^2$ and $\frac{\mathrm{d}}{\mathrm{d}t}\|\boldsymbol{x}(t)\|^2$,

$$\begin{aligned}\|\boldsymbol{x}(t)\| &= \sqrt{\|\boldsymbol{x}(t)\|^2} \\ \mathcal{R}_t^{\mathrm{ins}} &= -\frac{1}{2\,\|\boldsymbol{x}(t)\|^2}\frac{\mathrm{d}}{\mathrm{d}t}\|\boldsymbol{x}(t)\|^2 \\ \mathcal{R}_t^{\mathrm{avg}} &= -\frac{\ln\|\boldsymbol{x}(t)\|^2 - \ln\|\boldsymbol{x}(0)\|^2}{2t}. \end{aligned}$$

Applying these functions to the means of $\|\boldsymbol{x}(t)\|^2$ and $\frac{\mathrm{d}}{\mathrm{d}t}\|\boldsymbol{x}(t)\|^2$ (i.e., Eqs. (D.1) and (D.2)) gives poor approximations for the means of $\|\boldsymbol{x}(t)\|$, $\mathcal{R}_t^{\mathrm{ins}}$ and $\mathcal{R}_t^{\mathrm{avg}}$. Applying the same procedure to medians leads to much better approximations. Explicitly, denoting by $\mathbb{M}$ the median value over the perturbation vectors $\boldsymbol{u}$, we get from Eqs. (D.1) and (D.2),

$$\begin{aligned}\mathbb{M}\left(\|\boldsymbol{x}(t)\|^2\right) &\approx \mathrm{Tr}\,C\,\mathrm{e}^{A^\top t}\,\mathrm{e}^{At} \\ \mathbb{M}\left(\frac{\mathrm{d}}{\mathrm{d}t}\|\boldsymbol{x}(t)\|^2\right) &\approx 2\,\mathrm{Tr}\,C\,\mathrm{e}^{A^\top t}\,H(A)\,\mathrm{e}^{At}. \end{aligned}$$

Hence,

$$\mathbb{M}\left(\|\boldsymbol{x}(t)\|\right) \approx \sqrt{\mathrm{Tr}\left(C\,\mathrm{e}^{A^\top t}\,\mathrm{e}^{At}\right)} \tag{D.3}$$

$$\mathbb{M}\left(\mathcal{R}_t^{\mathrm{ins}}\right) \approx -\frac{\mathrm{Tr}\left(C\,\mathrm{e}^{A^\top t}\,H(A)\,\mathrm{e}^{At}\right)}{\mathrm{Tr}\left(C\,\mathrm{e}^{A^\top t}\,\mathrm{e}^{At}\right)} \tag{D.4}$$

$$\mathbb{M}\left(\mathcal{R}_t^{\mathrm{avg}}\right) \approx -\frac{\ln\left(\mathrm{Tr}\,C\,\mathrm{e}^{A^\top t}\,\mathrm{e}^{At}\right) - \ln\left(\mathrm{Tr}\,C\right)}{2t}. \tag{D.5}$$

The accuracy of the approximations is excellent, as illustrated in Figs. 2–4 and A.1 (compare full line (numerically computed median) and $\times$-marks (analytical approximation); Eq. (D.3) in panel C and Eq. (D.5) in panel D).

It is interesting to consider the median of initial return rate $\mathcal{R}_0^{\mathrm{ins}} = \lim_{t\to 0}\mathcal{R}_t^{\mathrm{avg}}$. From Eq. (D.4) or (D.5),

$$\mathbb{M}\left(\mathcal{R}_0^{\mathrm{ins}}\right) = \lim_{t\to 0}\mathbb{M}\left(\mathcal{R}_t^{\mathrm{avg}}\right) \approx -\frac{\mathrm{Tr}\left(CH(A)\right)}{\mathrm{Tr}\,C} = -\frac{\mathrm{Tr}\left(CA\right)}{\mathrm{Tr}\,C}.$$

In the simple case where C is proportional to the identity matrix (see next section), we find that

$$\mathbb{M}\left(\mathcal{R}_0^{\mathrm{ins}}\right) = \lim_{t\to 0}\mathbb{M}\left(\mathcal{R}_t^{\mathrm{avg}}\right) = -\frac{1}{n}\mathrm{Tr}\,A = -\frac{1}{n}\sum_{i=1}^{n}\lambda_i = \frac{1}{n}\sum_{i=1}^{n} -\Re\mathfrak{e}(\lambda_i),$$

where λ_i are the eigenvalues of A. Hence, the median initial return rate is always positive and larger than asymptotic resilience. This is the case even for reactive systems, for which the initial return rate for some perturbation directions is negative (that is, the system initially moves away from equilibrium).

A similar procedure as above can be used to derive approximations for the median values of $|\langle \boldsymbol{w}, \boldsymbol{x}(t)\rangle|$, $\mathcal{R}_t^{\mathrm{ins}}(\boldsymbol{w})$ and $\mathcal{R}_t^{\mathrm{avg}}(\boldsymbol{w})$,

$$\mathbb{M}\left(|\langle \boldsymbol{w}, \boldsymbol{x}(t)\rangle|\right) \approx \sqrt{\langle w|\,\mathrm{e}^{At}\,C\,e^{A^\top t}\,w\rangle} \tag{D.6}$$

$$\mathbb{M}\left(\mathcal{R}_t^{\mathrm{ins}}(\boldsymbol{w})\right) \approx -\frac{\langle w|\,\mathrm{e}^{At}\left(AC + CA^\top\right)\mathrm{e}^{A^\top t}w\rangle}{2\,\langle w|\,\mathrm{e}^{At}\,C\,e^{A^\top t}\,w\rangle} \tag{D.7}$$

$$\mathbb{M}\left(\mathcal{R}_t^{\mathrm{avg}}(\boldsymbol{w})\right) \approx -\frac{\ln\langle w|\,\mathrm{e}^{At}\,C\,e^{A^\top t}\,w\rangle - \ln\langle w|\,C\,w\rangle}{2t}. \tag{D.8}$$

The accuracy of these approximations is illustrated in Fig. B.1 (Eq. (D.6) in panel C and Eq. (D.8) in panel D).

Appendix E. Correlation matrix of perturbations

The statistics of the perturbation $\boldsymbol{u}$ acting on the system are summarized in the correlation matrix C. Here we derive this covariance matrix for two simple random perturbation models. In the first model we assume that all perturbation directions $\boldsymbol{u}$ are equally probable. This implies that on average all species are equally displaced. In the second model we allow that certain perturbation directions are more probable than others. In particular, we assume that a typical perturbation will displace more, in absolute terms, species with large equilibrium biomass.

To define the first model, we specify the distribution of the random perturbation vector $\boldsymbol{u}$. For a given perturbation direction (i.e., given $\boldsymbol{u}/\|\boldsymbol{u}\|$), the norm $\|\boldsymbol{u}\|$ of the perturbation vector has no effect on the return rates by linearity. Hence, we can choose $\|\boldsymbol{u}\| = 1$. Then, because all perturbation directions are equally probable, we see that the perturbation vector $\boldsymbol{u}$ is uniformly distributed on the unit sphere (i.e., the sphere defined by the condition $\|\boldsymbol{u}\| = 1$).

To generate samples from this distribution, the following procedure can be used,

1. Generate a vector $\boldsymbol{v}$, of the same dimension as $\boldsymbol{u}$, consisting of independent standard Gaussian variables v_i.
2. The normalized vector $\boldsymbol{u} = \boldsymbol{v}/\|\boldsymbol{v}\|$ gives a sample from the uniform distribution on the unit sphere.

Note that the components v_i of vector $\boldsymbol{v}$ have to be taken from a Gaussian distribution for this procedure to work. Hence, we have the following relationships between the probability distributions of $\boldsymbol{v}$, $\boldsymbol{u}$ and $r = \|\boldsymbol{v}\|$,

$$\mathbb{P}(\boldsymbol{v} \in \mathrm{d}\boldsymbol{v}) = \mathbb{P}(r \in \mathrm{d}r)\,\mathbb{P}(\boldsymbol{u} \in \mathrm{d}\boldsymbol{u}) = \prod_i \mathbb{P}(v_i \in \mathrm{d}v_i), \tag{E.1}$$

where the distributions $\mathbb{P}(v_i \in \mathrm{d}v_i)$ are standard Gaussian.

To compute the corresponding correlation matrix C, we start from the equality

$$C = \mathbb{E}\,|\boldsymbol{u}\rangle\langle\boldsymbol{u}| = \int |\boldsymbol{u}\rangle\langle\boldsymbol{u}|\,\mathbb{P}(\boldsymbol{u} \in \mathrm{d}\boldsymbol{u}). \tag{E.2}$$

We multiply both sides of the equation by r^2 and integrate with respect to distribution of $r = \|\boldsymbol{v}\|$. For the left-hand side, we get

$$\begin{aligned}\int C\, r^2\, \mathbb{P}(r \in \mathrm{d}r) &= C \int r^2\, \mathbb{P}(r \in \mathrm{d}r)\\ &= C \int \|v\|^2\, \mathbb{P}(\boldsymbol{v} \in \mathrm{d}\boldsymbol{v})\\ &= C \int \sum_i v_i^2 \prod_i \mathbb{P}(v_i \in \mathrm{d}v_i)\\ &= C \sum_i \int v_i^2\, \mathbb{P}(v_i \in \mathrm{d}v_i) = n\,C,\end{aligned}$$

where n is the dimension of $\boldsymbol{u}$ and $\boldsymbol{v}$. For the right-hand side, we get

$$\int |\boldsymbol{u}\rangle\langle\boldsymbol{u}|\,\mathbb{P}(\boldsymbol{u} \in \mathrm{d}\boldsymbol{u})\, r^2\, \mathbb{P}(r \in \mathrm{d}r) = \int |\boldsymbol{v}\rangle\langle\boldsymbol{v}|\,\mathbb{P}(\boldsymbol{v} \in \mathrm{d}\boldsymbol{v}).$$

Hence, we find that

$$C = \frac{1}{n} \int |\boldsymbol{v}\rangle\langle\boldsymbol{v}|\,\mathbb{P}(\boldsymbol{v} \in \mathrm{d}\boldsymbol{v}). \tag{E.3}$$

The integral in the right-hand side is equal to the correlation matrix of the random variables v_i. They are independent and have variance 1, so that

$$C = \frac{1}{n}\mathbb{1}, \tag{E.4}$$

where $\mathbb{1}$ denotes the $n \times n$ identity matrix.

To define the second model, we give the procedure to sample random perturbations $\boldsymbol{u}$. The procedure is a slightly modified version of the previous sampling procedure,

1. Generate a vector $\boldsymbol{v}$, of the same dimension as $\boldsymbol{u}$, consisting of independent standard Gaussian variables v_i.
2. Multiply the vector $\boldsymbol{v}$ by D, the diagonal matrix containing the equilibrium species biomass, giving $\boldsymbol{w} = D\boldsymbol{v}$.
3. The normalized vector $\boldsymbol{u} = \boldsymbol{w}/\|\boldsymbol{w}\|$ gives a sample from the distribution of perturbation $\boldsymbol{u}$.

Note that this is again a distribution on the unit sphere (defined by $\|\boldsymbol{u}\| = 1$). However, this distribution is not uniform due to the multiplication by matrix D.

We compute the corresponding correlation matrix C. First, we note that the components of vector $\boldsymbol{w}$ are independent Gaussian variables. Their distributions are not identical; component w_i has variance D_{ii}^2 (and mean 0). Introducing the variable $r = \|\boldsymbol{w}\|$, we have the following relationships,

$$\mathbb{P}(\boldsymbol{w} \in \mathrm{d}\boldsymbol{w}) = \mathbb{P}(r \in \mathrm{d}r)\,\mathbb{P}(\boldsymbol{u} \in \mathrm{d}\boldsymbol{u}) = \prod_i \mathbb{P}(w_i \in \mathrm{d}w_i), \tag{E.5}$$

Then, we can apply a similar computation as for the first model. Using that

$$\int r^2\,\mathbb{P}(r \in \mathrm{d}r) = \sum_i \int w_i^2\,\mathbb{P}(w_i \in \mathrm{d}w_i) = \sum_i D_{ii}^2,$$

we get

$$C = \frac{1}{\sum_i D_{ii}^2} \int |\boldsymbol{w}\rangle\langle\boldsymbol{w}|\,\mathbb{P}(\boldsymbol{w} \in \mathrm{d}\boldsymbol{w}). \tag{E.6}$$

The integral in the right-hand side is the covariance matrix of the random variables w_i. Substituting their variances and covariances, we find that

$$C = \frac{1}{\sum_i D_{ii}^2} D^2. \tag{E.7}$$

This result show that, on average, species with larger biomass are affected more strongly by the perturbation. The standard deviation of the displacement of species i is proportional to D_{ii}. Hence, the displacement strength relative to species biomass does not differ between species. Note that also for this second model the perturbation affects species in an uncorrelated way.

Appendix F. Effect of rare species on asymptotic resilience

Here we illustrate a simple mechanism of how a rare species can determine asymptotic resilience. We assume that the rare species is present in the community without significantly affecting the other species, but is kept at low abundance by interactions with the core community (a satellite species). We consider two cases: one in which the rare species can persist in the community without immigration, and another in which the rare species is maintained by immigration (a sink population).

We focus on the dynamics of the satellite species, which we describe by logistic growth with immigration. Denoting its biomass by N_1, the dynamical equation reads,

$$\frac{\mathrm{d}N_1}{\mathrm{d}t} = r_1 N_1 \left(1 - \frac{N_1 + \beta_{10} N_0}{K_1}\right) + c_1, \tag{F.1}$$

with r_1 the intrinsic growth rate, K_1 the carrying capacity, and c_1 the immigration rate of the satellite species. Variable N_0 aggregates the biomass of the core species. Because the effect of the satellite species on the core species is assumed to be negligible, the dynamics of N_0 are autonomous, converging to an equilibrium value N_0^*. Competition coefficient β_{10} quantifies the negative effect of the core species on the satellite species, effectively reducing its intrinsic growth rate,

$$r_1 \;\rightarrow\; r_1\left(1 - \frac{\beta_{10} N_0^*}{K_1}\right) = \alpha_1 r_1 \quad \text{with} \quad \alpha_1 = 1 - \frac{\beta_{10} N_0^*}{K_1}. \tag{F.2}$$

The factor α_1 is smaller than one, and can even be negative. The effective growth rate $\alpha_1 r_1$ is equal to the invasion fitness of the satellite species (without immigration).

First, assume the satellite species has positive invasion fitness, $\alpha_1 > 0$, so that it can persist in the community without immigration. Neglecting immigration, $c_1 = 0$, we find that the equilibrium biomass is $N_1^* = \alpha_1 K_1$ and that the corresponding eigenvalue is $-\alpha_1 r_1$ (recall that the other eigenvalues of the community dynamics are basically unaffected by the satellite species). Hence, for small α_1, the satellite species contributes a small eigenvalue (in absolute value). The eigenvalue might be smaller than the other eigenvalues of the community dynamics, in which case the satellite species determines asymptotic resilience.

Second, assume the satellite species has negative invasion fitness, $\alpha_1 < 0$, so that it is maintained in the community by immigration. Neglecting intraspecific competition (i.e., dropping the N_1^2 term in Eq. (F.1)), we obtain the equilibrium biomass $N_1^* = c_1/(|\alpha_1| r_1)$ and the corresponding eigenvalue $\alpha_1 r_1$. If immigration is very weak (very small c_1), both biomass and eigenvalue can be small. Hence, the satellite species can contribute a weakly negative eigenvalue to the community dynamics, and might even determine asymptotic resilience.

The two cases (positive and negative invasion fitness) are illustrated in Fig. 5. For concreteness, we complement Eq. (F.1) with a simple dynamical equation for the aggregate biomass N_0,

$$\frac{\mathrm{d}N_0}{\mathrm{d}t} = r_0 N_0 \left(1 - \frac{N_0}{K_0}\right). \tag{F.3}$$

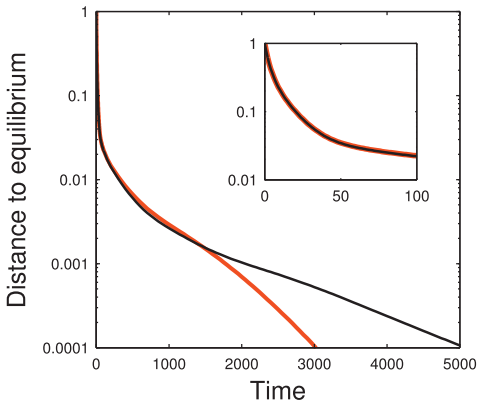

Fig. F.1. Rare species determine asymptotic resilience in random community model. Same model as in Fig. 6, but here we look at a single realization. Black line: recovery trajectory for full community (averaged over perturbation directions). Red line: recovery trajectory for community from which the rarest species has been removed. Inset: zoom of the recovery trajectories for shorter times.

We take $r_0 = 1.0$ and $K_0 = 1.0$, so that $N_0^* = 1.0$ and the associated eigenvalue $\lambda_0 = -1.0$. For the satellite species we set $r_1 = 1.0$ and $\beta_{10} = 0.8$.

In case A of Fig. 5, we take $K_1 = 0.77$ and $c_1 = 0$, so that $\alpha_1 = -0.039$. Hence, the satellite species cannot persist and the community dynamics are not affected.

In case B of Fig. 5, we take $K_1 = 0.83$ and $c_1 = 0$, so that $\alpha_1 = 0.036$. Hence, the satellite species can persist and its equilibrium biomass is $N_1^* = 0.030$. This introduces a new eigenvalue in the community dynamics, equal to $-0.036 = 0.036\,\lambda_0$, which is strongly dominant. This illustrates the first case discussed above.

In case C of Fig. 5, we take $K_1 = 0.77$ and $c_1 = 0.002$. The satellite species is maintained by immigration and its equilibrium biomass is $N_1^* = 0.027$. The associated eigenvalue $-0.11 = 0.11\,\lambda_0$ is strongly dominant. This illustrates the second case discussed above.

The previous observations can be generalized to many-species communities, as shown in Fig. 6. Here we look more closely at a single model realization (Fig. F.1). In this example, asymptotic resilience can be linked to a single species, because the left eigenvector associated with the dominant eigenvalue is strongly concentrated on a single component. This species is the rarest of the community. When removing this species, asymptotic resilience changes drastically, but the short-term recovery dynamics do not (see inset in Fig. F.1). The same phenomena are observed in a majority of model realizations. In other cases, asymptotic resilience is not as clearly associated with a single rare species.

References

Arnoldi, J.-F., Loreau, M., Haegeman, B., 2016. Resilience, reactivity and variability: a mathematical comparison of ecological stability measures. J. Theor. Biol. 389, 47–59.

Bender, E.A., Case, T.J., Gilpin, M.E., 1984. Perturbation experiments in community ecology: theory and practice. Ecology 65, 1–13.

Brose, U., Williams, R.J., Martinez, N.D., 2006. Allometric scaling enhances stability in complex food webs. Ecol. Lett. 9, 1228–1236.

Caswell, H., 2001. Matrix Population Models: Construction, Analysis and Interpretation. Sinauer Associates.

Caswell, H., 2007. Sensitivity analysis of transient population dynamics. Ecol. Lett. 10, 1–15.

Donohue, I., Hillebrand, H., Montoya, J.M., et al., 2016. Navigating the complexity of ecological stability. Ecol. Lett. 19, 1172–1185.

Donohue, I., Petchey, O.L., Montoya, J.M., et al., 2013. On the dimensionality of ecological stability. Ecol. Lett. 16, 421–429.

Downing, A.L., Leibold, M.A., 2010. Species richness facilitates ecosystem resilience in aquatic food webs. Freshwater Biol. 55 (10), 2123–2137.

Ezard, T.H., Bullock, J.M., Dalgleish, H.J., et al., 2010. Matrix models for a changeable world: the importance of transient dynamics in population management. J. Appl. Ecol. 47, 515–523.

Gellner, G., McCann, K.S., 2016. Consistent role of weak and strong interactions in high-and low-diversity trophic food webs. Nat. Commun. 7, 11180.

Grimm, V., Wissel, C., 1997. Babel, or the ecological stability discussions: an inventory and analysis of terminology and a guide for avoiding confusion. Oecologia 109, 323–334.

Gunderson, L.H., 2000. Ecological resilience – in theory and application. Ann. Rev. Ecol. Syst. 31, 425–439.

Gurney, W., Nisbet, R.M., 1998. Ecological Dynamics. Oxford University Press.

Haegeman, B., Arnoldi, J.-F., Wang, S., et al., 2016. Resilience, invariability, and ecological stability across levels of organization. bioRxiv 085825.

Hanski, I., 1982. Dynamics of regional distribution: the core and satellite species hypothesis. Oikos 38, 210–221.

Hastings, A., 2004. Transients: the key to long-term ecological understanding? Trends Ecol. Evol. 19, 39–45.

Hastings, A., 2010. Timescales, dynamics, and ecological understanding. Ecology 91, 3471–3480.

Holling, C.S., 1973. Resilience and stability of ecological systems. Ann. Rev. Ecol. Syst. 4, 1–23.

Hoover, D.L., Knapp, A.K., Smith, M.D., 2014. Resistance and resilience of a grassland ecosystem to climate extremes. Ecology 95 (9), 2646–2656.

Ives, A.R., Carpenter, S.R., 2007. Stability and diversity of ecosystems. Science 317, 58–62.

Loeuille, N., 2010. Influence of evolution on the stability of ecological communities. Ecol. Lett. 13, 1536–1545.

Lundström, N.L.P., 2017. How to find simple nonlocal stability and resilience measures. arXiv 1706.05689.

MacArthur, R.H., 1957. On the relative abundance of bird species. Proc. Natl. Acad. Sci. U.S.A. 43, 293–295.

May, R.M., 1973. Stability and Complexity in Model Ecosystems. Princeton Univ. Press.

May, R.M., 1974. Ecosystem patters in randomly fluctuating environments. In: Rosen, R., Snell, F.M. (Eds.), Progress in Theoretical Biology. Acadamic Press, New York, pp. 1–50.

McCann, K., Hastings, A., Huxel, G.R., 1998. Weak trophic interactions and the balance of nature. Nature 395 (6704), 794–798.

McCann, K.S., 2011. Food Webs. Princeton Univ. Press.

Menck, P.J., Heitzig, J., Marwan, N., Kurths, J., 2013. How basin stability complements the linear-stability paradigm. Nat. Phys. 9 (2), 89–92.

Neubert, M.G., Caswell, H., 1997. Alternatives to resilience for measuring the responses of ecological systems to perturbations. Ecology 78, 653–665.

Pimm, S.L., 1984. The complexity and stability of ecosystems. Nature 307, 321–326.

Pimm, S.L., Lawton, J.H., 1977. Number of trophic levels in ecological communities. Nature 268, 329–331.

Pimm, S.L., Lawton, J.H., 1978. On feeding on more than one trophic level. Nature 275, 542–544.

Rooney, N., McCann, K., Gellner, G., Moore, J.C., 2006. Structural asymmetry and the stability of diverse food webs. Nature 442, 265–269.

Steiner, C., Long, Z., Krumins, J., Morin, P., 2006. Population and community resilience in multitrophic communities. Ecology 87, 996–1007.

Stott, I., Townley, S., Hodgson, D.J., 2011. A framework for studying transient dynamics of population projection matrix models. Ecol. Lett. 14, 959–970.

Sugihara, G., 1980. Minimal community structure: an explanation of species abundance patterns. Am. Nat. 116, 770–787.

Thébault, E., Fontaine, C., 2010. Stability of ecological communities and the architecture of mutualistic and trophic networks. Science 329, 853–856.

Tilman, D., Downing, J., 1994. Biodiversity and stability in grasslands. Nature 367, 363–365.

Wright, A.J., Ebeling, A., de Kroon, H., et al., 2015. Flooding disturbances increase resource availability and productivity but reduce stability in diverse plant communities. Nat. Commun. 6, 6092.